Maps generated by entangled momenta: exploring spin entanglement in relativity

Article (Accepted Version)

Maps generated by entangled momenta: exploring spin entanglement in relativity

Veiko Palge,[1,*] Jacob Dunningham,[2,†] Stefan Groote,[1,‡] and Hannes Liivat[1,§]

[1]*Laboratory of Theoretical Physics, Institute of Physics, University of Tartu, W. Ostwaldi 1, 50411 Tartu, Estonia*

[2]*Department of Physics and Astronomy, University of Sussex, Brighton BN1 9QH, United Kingdom*

We study relativistic entanglement of a bipartite system consisting of massive spin-$1/2$ particles with momenta. The spin state is described by the maximally entangled Bell state and momenta are given by entangled Gaussian distributions. We conceptualize the dependency between spin and momentum in relativity along the lines of controlled operations in quantum information theory. This leads to a systematic study of maps that Wigner rotations generate on the spin degree of freedom of the total system in different boost scenarios. We use a visualization tool from quantum information theory in order to get better insight into how and why the entanglement changes in different boost geometries.

I. INTRODUCTION

While relativistic quantum theory is commonplace, relativistic quantum information theory, which seeks to provide a relativistic account of quantum information, has gradually risen in the last fifteen years or so. The core notion of quantum information is entanglement, the phenomenon that has been proven extremely useful for applications. Therefore, one of the central challenges of relativistic quantum information is the characterization of entanglement in relativity. The first studies on the subject appeared more than a decade ago [1–17] and the overall conclusion emerging is that relativistic entanglement in both inertial and accelerated frames is observer dependent [18].

The issue has been in the foreground since early on. A number of different results have been reported [2, 4, 19–23], some of which confirm the invariance of entanglement while others claim that entanglement depends on the boost in question. Analyzing the situation reveals that these findings commonly involve different momentum states and boost angles, or geometries. The study of the simplest system, the single particle [17], which can be viewed as playing the role of a relativistic qubit, also suggests that geometry has an important role to play. Along the same lines, the literature on the Wigner rotation is quite clear about the fact that its nature is highly geometric, yet except from a few cases [24] there is little work that systematically takes this into account.

These considerations lead to question that we would like to explore in the paper: what part have geometry and momentum states to play in determining the behavior of entanglement in relativity? In order to address the issue, we will focus on a system of two spin-$1/2$ particles and view them as two relativistic qubits. This enables to clarify the role of momenta and geometry as we will explain shortly. The idea is that boosts can be thought of as generating maps on spins, with momenta and geometry determining the extent to which the entanglement will change under boosts. While previous work has investigated systems with discrete momenta, our aim here is to study realistic systems whose momentum states are given by Gaussian distributions. We will thus assume that the momenta are given by entangled Gaussians while the spin degree of freedom is in a maximally entangled Bell state. In order to get a deeper insight into how and why the entanglement changes under boosts we will visualize the spin state in a 3D manner. We will also use a simple discrete model to help explain the various results obtained for the states with continuous momenta. Our hope is that such a survey contributes to a systematic study of how geometry and momenta influence the behavior of relativistic spin entanglement.

We begin by explaining the setup of our two particle system. The question of the relativistic spin observable is discussed in section III. Thereafter we explain how the spin state can be visualized for the so called Bell-diagonal states. The properties of Wigner rotation will then be reviewed, followed by the specification of the models we will study below. Section VII gives a detailed characterization of the momentum and spin states of the models. The second half of the paper from section VIII onwards examines how spin entanglement changes in two particle systems containing various forms of entangled momenta. The results will be summarized in section XII.

II. PHYSICAL SETUP

We will focus on a system consisting of two massive spin-$1/2$ particles and ask how the entanglement of the spin degree of freedom changes when viewed from a different inertial frame. This question is interesting since in relativity the spin seen by an observer in any other frame generally depends on the momentum of the particle and the state of the observer. As a result, the spin entanglement in general changes nontrivially too. We begin the discussion by fixing the state space and calculating the generic transformation of a two particle state under Lorentz transformations.

However, before embarking on the analysis of two particle systems, it is worth clarifying what happens to a single particle system. The reason is that the mechanism that produces spin-spin entanglement in two particles originates in the behavior of the single particle. The single particle can be viewed as

* Email: veiko.palge@ut.ee
† Email: J.Dunningham@sussex.ac.uk
‡ Email: stefan.groote@ut.ee
§ Email: hannes.liivat@ut.ee

forming a 'qubit' of relativistic massive spin-$1/2$ systems in inertial frames. A generic state $|\Psi\rangle \in \mathcal{H}_1$ for observer O can be written as

$$|\Psi\rangle = \sum_\lambda \int \mathrm{d}\mu(p)\, \psi_\lambda(\mathbf{p})\, |\mathbf{p},\lambda\rangle, \tag{1}$$

where $|\mathbf{p},\lambda\rangle \equiv |\mathbf{p}\rangle\,|\lambda\rangle \equiv |\mathbf{p}\rangle \otimes |\lambda\rangle$ are basis vectors in the Wigner representation (also called the Wigner-Bargmann or the spin basis [25]) which we will use throught the paper, $\mathbf{p}$ labels the single particle momentum, $\lambda = \pm\frac{1}{2}$ is the spin and $\mathcal{H}_1 = L^2(\mathbb{R}^3) \otimes \mathbb{C}^2$ stands for the single particle state space (see Appendix A for constructions used in the paper). An observer O^Λ Lorentz boosted by Λ assigns the same system a different wave function

$$\psi_\lambda(\mathbf{p}) \mapsto \psi^\Lambda_\lambda(\mathbf{p}) = \sum_\sigma D_{\lambda\sigma}[W(\Lambda,\Lambda^{-1}\mathbf{p})]\psi_\sigma(\Lambda^{-1}\mathbf{p}), \tag{2}$$

where $D[W(\Lambda,\mathbf{p})]$ is the representation of the Wigner, or Thomas–Wigner rotation (TWR), $W(\Lambda,\mathbf{p})$ [26]. This means that for O^Λ the spin appears rotated by $D[W(\Lambda,\mathbf{p})]$, and the rotation depends on the geometry, i.e. the angle between two boosts as well as the the momenta of the system and the observer. As an interesting implication, note that this means that states whose spin and momentum are separable for observer O may display spin–momentum entanglement to the moving observer O^Λ, see for example [3, 17].

The peculiar dependency of spin on momentum can be viewed in terms of an analogy from quantum information theory [2, 3]. Consider the so-called controlled unitary gate. It has two input qubits which are called the control qubit and the target qubit. The action of the gate is to transform the target qubit with a unitary transformation U depending on the control qubit. One can think of the Lorentz boost along the same lines. If momentum takes the role of a control qubit, then if the boost angle and rapidity are fixed, the transform on the spin state depends only on the momentum state. Although we will not use this in calculations, the idea of Lorentz boosts as controlled unitaries is the principle that guides our investigation of the relativistic spin–momentum systems in this paper.

Let us now consider a two particle system, the system that we will be studying in what follows. A generic pure state $|\Psi\rangle \in \mathcal{H}_1 \otimes \mathcal{H}_1$ can be written as follows,

$$|\Psi\rangle = \sum_{\lambda\eta} \int \mathrm{d}\mu(p,q)\, \psi_{\lambda\eta}(\mathbf{p},\mathbf{q})\, |\mathbf{p},\lambda\rangle\, |\mathbf{q},\eta\rangle, \tag{3}$$

where we have abbreviated $\mathrm{d}\mu(p,q) = \mathrm{d}\mu(p)\mathrm{d}\mu(q)$ and $\mathcal{H}_1$ is again the single particle state space. Boost Λ induces a transformation of the wave function for O^Λ (see Appendix A for details),

$$\psi^\Lambda_{\lambda\kappa}(\mathbf{p},\mathbf{q}) = \sum_{\sigma,\xi} D_{\lambda\sigma}\big[W(\Lambda,\Lambda^{-1}\mathbf{p})\big]\, D_{\kappa\xi}\big[W(\Lambda,\Lambda^{-1}\mathbf{q})\big] \times \psi_{\sigma\xi}(\Lambda^{-1}\mathbf{p},\Lambda^{-1}\mathbf{q}). \tag{4}$$

Each spin undergoes a momentum dependent rotation which induces a non-trivial transformation on the spin degree of freedom of the total two particle state. In other words, boosts generally change the spin-spin entanglement of the total system. Notice how the single particle system forms the primitive building block whose behavior under boosts leads to more complex behavior in the larger system of two particles. The mechanism that leads to *spin-momentum* entanglement in single particle systems is precisely the one that causes non-trivial changes in the *spin-spin* entanglement of two particles.

Returning to the qubit analogy, we can think of the two particle system as consisting of two control qubits, i.e. the two momenta, and two target qubits, i.e. the two spins. Choosing a particular momentum state means boosts will induce a specific transformation on the target spins. One can now pose the question of what are the maps that different kinds of momentum states generate on spins? This is a wide ranging question which cannot be addressed in a single paper. Instead we will adopt a piecemeal approach and probe spin entanglement with a subset of interesting momenta. In particular, we have learned from quantum information theory that entangled states lead to phenomena which are distinctive to the quantum realm. Motivated by this, we will ask what are the transformations that entangled momenta generate on the (maximally) entangled spin state of a two particle system [27]? Furthermore, while previous work has investigated systems with discrete momenta [28], which represent idealized models, realistic situations involve states whose momenta are given by continuous distributions. In order to understand how relaxing idealization affects the behavior of entanglement we will assume that momenta are given by entangled states that consist of combinations of Gaussians.

III. SPIN OBSERVABLE

Treatment of spin in relativity is somewhat more complicated than in the non-relativistic theory. This is due to the fact that the commutation relation of two generators of rotationless Lorentz boosts results in a rotation generator, $[K_i, N_j] = -i\epsilon_{ijk}J_k$. The latter is the infinitesimal algebraic form of the TWR. It means that two non-collinear rotationless Lorentz boosts will generate a rotation. From the geometric point of view it is interesting to note that the same phenomenon is related to the fact that the relativistic momentum space, the mass shell hyperbola, is a curved space: a Riemannian space with constant negative curvature [29].

While there is some controversy about what is the most adequate spin operator in the relativistic quantum theory, one candidate stands out. It is the so-called Newton-Wigner spin observable, which has advantages over other spins because it possesses a number of properties one naturally demands of a good spin operator. We will give a brief summary of the reasoning that leads to the Newton-Wigner spin. A good overview along with the discussion of the various spin candidates can be found in [25].

Relativistic quantum theory conceptualizes particles as group representations. Elementary particles correspond to the unitary irreducible representations of the Poincaré group, which are characterized by two labels, mass m and spin s. Mass is given by the square root of the eigenvalues of the

first Casimir invariant, the mass square operator $P^2 = P_\mu P^\mu$. Spin is related to the eigevalues of the second Casimir invariant, $W^2 = W_\mu W^\mu$, where

$$W^\mu = \frac{1}{2}\epsilon^{\nu\alpha\beta\mu} P_\nu J_{\alpha\beta} \tag{5}$$

is the Pauli-Lubanski vector and $J_{\alpha\beta}$ are the generators of the Lorentz group. The components of $W = (W^0, W^j)$ are given by

$$\begin{aligned} W^0 &= P^j M^j = \mathbf{P}\cdot\mathbf{M}, \\ W^j &= P^0 M^j - \epsilon^{jkl} P^k N^l = P^0 M^j - (\mathbf{P}\times\mathbf{N})^j. \end{aligned} \tag{6}$$

One can then define the spin square operator as

$$\mathbf{S}^2 = -\frac{1}{m^2} W_\mu W^\mu. \tag{7}$$

This leads to the idea that the spin operator can be postulated as a linear combination of the components of W given that certain conditions are satisifed, conditions that one would reasonably require of a spin observable. These are as follows, (i) the spin operator $\mathbf{S}$ should fulfill the usual commutation relations,

$$[S^i, S^j] = \mathrm{i}\epsilon_{ijk} S^k, \tag{8}$$

(ii) it is a three dimensional vector, that is

$$[J^i, S^j] = \mathrm{i}\epsilon_{ijk} S^k, \tag{9}$$

and (iii) in any frame the vector $\mathbf{S}$ is a linear combination of components of W with coefficients that depend only on the four momentum P^μ. It can be shown that there is a unique linear combination of operators W^μ which satisfies these conditions and it has the form [30],

$$\mathbf{S}_{\mathrm{NW}} = \frac{1}{m}\left(\mathbf{W} - \frac{W_0}{m + P^0}\mathbf{P}\right). \tag{10}$$

The Newton-Wigner observable corresponds to the Pauli-Lubanski vector which is boosted to the rest frame of the particle [31],

$$(\mathbf{S}_{\mathrm{NW}})^j = \frac{1}{m}\left(L_p^{-1} W\right)^j, \tag{11}$$

where L_p^{-1} is the boost that takes momentum p to the rest system of the particle, $L_p^{-1} p = (m, 0, 0, 0)$. We will use the Newton-Wigner spin observable $\mathbf{S}_{\mathrm{NW}}$ throughout the paper to characterize the spin of the particles.

Since we are working in the Wigner representation, we need to express $\mathbf{S}_{\mathrm{NW}}$ in that representation. The canonical form of the infinitesimal generators P^μ, $\mathbf{M}$ and $\mathbf{N}$ is as follows [31],

$$\begin{aligned} P^\mu &= p^\mu, \\ \mathbf{M} &= -i\mathbf{p}\times\partial_{\mathbf{p}} + \mathbf{S}, \\ \mathbf{N} &= -ip^0\partial_{\mathbf{p}} - \frac{\mathbf{p}\times\mathbf{S}}{m + p^0}, \end{aligned} \tag{12}$$

where $\mathbf{S} = \frac{1}{2}\boldsymbol{\sigma}$ and $\boldsymbol{\sigma} = (\sigma_x, \sigma_y, \sigma_z)$ are the Pauli matrices. Substituting the generators (12) into (6) and (10), we obtain for the Newton-Wigner observable

$$\mathbf{S}_{\mathrm{NW}} = \frac{1}{2}\boldsymbol{\sigma}, \tag{13}$$

meaning that in the Wigner representation $\mathbf{S}_{\mathrm{NW}}$ is given by the standard Pauli matrices.

IV. ENTANGLEMENT

In order to determine how the entanglement of the spin degree of freedom changes in various boost scenarios, we will calculate the boosted spin state ρ_S^Λ. The two particle spin state can be written in the operator basis

$$\rho_S^\Lambda = \frac{1}{4}\left(\mathbb{1}\otimes\mathbb{1} + \mathbf{r}\boldsymbol{\sigma}\otimes\mathbb{1} + \mathbb{1}\otimes\mathbf{s}\boldsymbol{\sigma} + \sum_{i,j} t_{ij}\sigma_i\otimes\sigma_j\right), \tag{14}$$

where the coefficients $\mathbf{r} = (r_x, r_y, r_z)$, $\mathbf{s} = (s_x, s_y, s_z)$ and t_{ij}, $i, j \in \{x, y, z\}$ are the expectation values of the spin observables $\boldsymbol{\sigma}\otimes\mathbb{1}$, $\mathbb{1}\otimes\boldsymbol{\sigma}$ and $\sigma_i\otimes\sigma_j$. Since the total state of two particles includes momentum as well, i.e. it lives in the space

$$\mathcal{H}_p^1 \otimes \mathcal{H}_\lambda^1 \otimes \mathcal{H}_p^2 \otimes \mathcal{H}_\lambda^2, \tag{15}$$

the expectation values of observables have the form

$$\begin{aligned} \langle\mathbf{r}\rangle &= \mathrm{Tr}\left(\rho^\Lambda\, \mathbb{1}_p^1\otimes\mathbf{S}_{\mathrm{NW}}^1\otimes\mathbb{1}_p^2\otimes\mathbb{1}_\sigma^2\right), \\ \langle\mathbf{s}\rangle &= \mathrm{Tr}\left(\rho^\Lambda\, \mathbb{1}_p^1\otimes\mathbb{1}_\sigma^1\otimes\mathbb{1}_p^2\otimes\mathbf{S}_{\mathrm{NW}}^2\right), \\ \langle t_{ij}\rangle &= \mathrm{Tr}\left(\rho^\Lambda\, \mathbb{1}_p^1\otimes\mathbf{S}_{\mathrm{NW}}^1\otimes\mathbb{1}_p^2\otimes\mathbf{S}_{\mathrm{NW}}^2\right), \end{aligned} \tag{16}$$

where the superscripts denote the first and the second particle, respectively, and $\rho^\Lambda = \left|\Psi^\Lambda\right\rangle\left\langle\Psi^\Lambda\right|$.

Since the final spin state ρ^Λ is generally mixed, we will use concurrence $C(\rho)$ to quantify the entanglement of spins. Concurrence of a bipartite state ρ of two qubits is defined as

$$C(\rho) = \max\{0, \lambda_1 - \lambda_2 - \lambda_3 - \lambda_4\}, \tag{17}$$

where the λ_i are square roots of eigenvalues of a non-Hermitian matrix $\rho\widetilde{\rho}$ in decreasing order and

$$\widetilde{\rho} = (\sigma_y\otimes\sigma_y)\,\rho^*\,(\sigma_y\otimes\sigma_y), \tag{18}$$

with σ_y a Pauli matrix, is the spin-flipped state with the complex conjugate * taken in the standard basis [32].

V. VISUALIZATION OF SPIN STATE

We will next characterize the spin state of the system. Most previous work has focussed on the Bell states,

$$|\Phi_\pm\rangle = \frac{1}{\sqrt{2}}\left(|00\rangle \pm |11\rangle\right), \quad |\Psi_\pm\rangle = \frac{1}{\sqrt{2}}\left(|01\rangle \pm |10\rangle\right), \tag{19}$$

the maximally entangled bipartite states of two level systems. Understanding their behavior in relativity is important for quantum information and we will follow suit in this paper [33]. As regards the geometric configuration, we will assume throughout that the spins are aligned with the z-axis irrespective of the direction of the boost. We adopt the convention that $|0\rangle$ signifies the 'up' spin and $|1\rangle$ the 'down' spin.

In order to gain a better understanding of the state change of a single qubit, one commonly uses visualization in terms of the Bloch sphere. Visualization of two qubits, however, is in general impossible since one needs 15 real parameters to characterize the density matrix. However, some cases still allow for a representation in three space, for instance when the state is restricted to evolve in a subspace of few dimensions. Fortunately this turns out to be the case for our system.

It is useful to work in the Hilbert-Schmidt space of operators $B(\mathcal{H})$, defined on the Hilbert space $\mathcal{H}$ with $\dim = N$ [34]. $B(\mathcal{H})$ becomes a Hilbert space of N^2 complex dimensions when equipped with a scalar product defined as $\langle A|B\rangle = \mathrm{Tr}(A^\dagger B)$, with $A, B \in B(\mathcal{H})$, where the squared norm is $\|A\|^2 = \mathrm{Tr}(A^\dagger A)$. The vector space of Hermitian operators is an N^2 real-dimensional subspace of Hilbert-Schmidt space which can be coordinatized using a basis that consists of identity operator and the generators of $\mathrm{SU}(N)$. For a qubit $N = 2$ and we obtain the familiar Bloch ball. For a bipartite qubit system $N = 4$, $B(\mathcal{H}) = B(\mathcal{H}_A)\otimes B(\mathcal{H}_B)$ where $\mathcal{H}_i$ is the single particle space, and we can use a basis whose elements are the tensor products $\{\mathbb{1}\otimes\mathbb{1}, \mathbb{1}\otimes\boldsymbol{\sigma}, \boldsymbol{\sigma}\otimes\mathbb{1}, \boldsymbol{\sigma}\otimes\boldsymbol{\sigma}\}$, where $\boldsymbol{\sigma} = (\sigma_x, \sigma_y, \sigma_z)$ is the vector of Pauli operators. The density operator for a 2×2 dimensional system can be written in the general form (14) where the coefficients $\mathbf{r}$, $\mathbf{s}$ and $t_{ij}, i, j \in \{x, y, z\}$ are the expectation values of the operators $\boldsymbol{\sigma}\otimes\mathbb{1}$, $\mathbb{1}\otimes\boldsymbol{\sigma}$ and $\sigma_i\otimes\sigma_j$.

For the projectors on the Bell states $s_i = r_i = 0$ and the matrix t_{ij} is diagonal. This implies we only need to consider the values of diagonal components t_{ii} which constitute a vector in 3-dimensional space, allowing us to represent the states in Euclidean three space [35]. The Bell states correspond to vectors,

$$\begin{aligned} t_{\Phi_+} &= (1,-1,\ \ 1)\,, & t_{\Phi_-} &= (-1,\ \ 1,\ \ 1)\,,\\ t_{\Psi_+} &= (1,\ \ 1,-1)\,, & t_{\Psi_-} &= (-1,-1,-1)\,, \end{aligned} \tag{20}$$

which, in turn, correspond to the vertices of a tetrahedron $\mathcal{T}$ in Fig. 1. By taking convex combinations of these, one obtains further diagonal states; the set of all such states is called *Bell-diagonal* and is represented by the (yellow) tetrahedron $\mathcal{T}$ in Fig. 1. The set of separable states forms a double pyramid, an octahedron, in the tetrahedron. The octahedron is given by the intersection of $\mathcal{T}$ with its reflection through the origin, $-\mathcal{T}$. The maximally mixed state $\frac{1}{4}\mathbb{1}_4$ has coordinates $(0,0,0)$ and it lies at the origin. The entangled states are located outside the octahedron in the cones of the tetrahedron, see Fig. 1.

We can now visualize the behavior of spin by calculating the coefficients t_{ii} under a given rotation as a function of rapidity ξ,

$$t(\xi) = (t_{xx}, t_{yy}, t_{zz})\,, \tag{21}$$

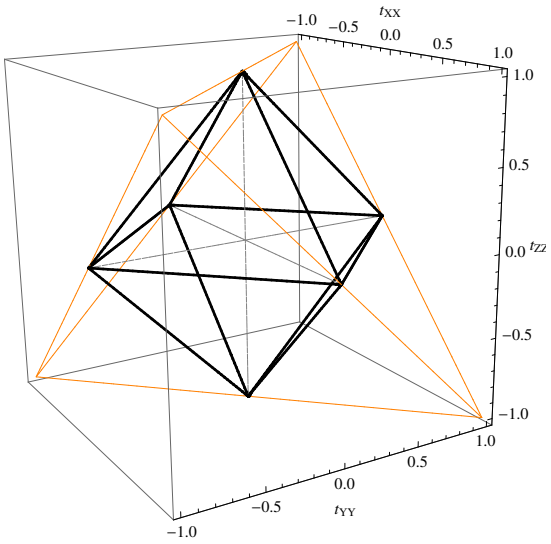

Figure 1. The geometry of Bell diagonal states. The vertices of the tetrahedron $\mathcal{T}$ (yellow) correspond to the four Bell states $|\Phi_+\rangle$, $|\Phi_-\rangle$, $|\Psi_+\rangle$, and $|\Psi_-\rangle$. Convex combinations of projectors on the Bell states, the Bell diagonal states, lie on or in the tetrahedron. A Bell diagonal state is separable iff it lies in the double pyramid formed by the intersection of the tetrahedron $\mathcal{T}$ and its reflection through the origin $-\mathcal{T}$.

where

$$t_{ii} = \mathrm{Tr}\big[\rho_S^\Lambda(\xi)\,\sigma_i\otimes\sigma_i\big]\,, \quad i\in\{x,y,z\}, \tag{22}$$

and $\rho_S^\Lambda(\xi)$ is the boosted spin state. The resulting set of three vectors

$$\Gamma\big[\rho_S^\Lambda(\xi)\big] = \{t(\xi)\mid \xi\in[0,\xi_{\max}]\} \tag{23}$$

we call an *orbit* of a given initial state. It can be represented as a curve in three space in the manner described above.

VI. THOMAS–WIGNER ROTATION

The TWR arises from the fact that the subset of Lorentz boosts does not form a subgroup of the Lorentz group. Consider three inertial observers O, O' and O'' where O' has velocity $\mathbf{v}_1$ relative to O and O'' has $\mathbf{v}_2$ relative to O'. Then the combination of two canonical boosts $\Lambda(\mathbf{v}_1)$ and $\Lambda(\mathbf{v}_2)$ that relates O to O'' is in general a boost *and* a rotation,

$$\Lambda(\mathbf{v}_2)\Lambda(\mathbf{v}_1) = R(\omega)\Lambda(\mathbf{v}_3), \tag{24}$$

where $R(\omega)$ is the TWR with angle ω. To an observer O, the frame of O'' appears to be rotated by ω. We will immediately specialize to massive systems, then $R(\omega)\in\mathrm{SO}(3)$ and ω is given by [36, 37]

$$\tan\frac{\omega}{2} = \frac{\sin\theta}{\cos\theta + D}, \tag{25}$$

where θ is the angle between two boosts or, equivalently, $\mathbf{v}_1$ and $\mathbf{v}_2$, and

$$D = \sqrt{\left(\frac{\gamma_1+1}{\gamma_1-1}\right)\left(\frac{\gamma_2+1}{\gamma_2-1}\right)}, \tag{26}$$

with $\gamma_{1,2} = (1 - v_{1,2}^2)^{-1/2}$ and $v_{1,2} = |\mathbf{v}_{1,2}|$. We assume natural units throughout, $\hbar = c = 1$. The axis of rotation specified by $\mathbf{n} = \mathbf{v}_2 \times \mathbf{v}_1/|\mathbf{v}_2 \times \mathbf{v}_1|$ is orthogonal to the plane defined by $\mathbf{v}_1$ and $\mathbf{v}_2$. Using rapidity $\xi_{1,2} = \operatorname{arctanh} |\mathbf{v}_{1,2}|$ to represent the magnitude of the boost and subsuming both under a single parameter $\xi = \xi_1 = \xi_2$, we show the dependence of the TWR on the boost angle θ and ξ in Fig. 2. Two interesting characteristics are immediately noticeable. First, for any two boosts at a fixed angle θ, the TWR angle ω increases with ξ, approaching a maximum value as boosts approach the speed of light. Second, the angle θ at which the maximum TWR occurs depends on the magnitude of ξ. It is worth noting that ω approaches the maximum value 180° when boosts are almost opposite and approach the speed of light. At lower boost magnitudes, maximum rotation occurs earlier.

VII. THE MODEL: MOMENTA AND SPIN ROTATIONS

In this section, we will give a characterization of the models to be studied below. We will assume throughout that initially the spin and momentum degrees of freedom factorize,

$$|\Psi\rangle = \int \mathrm{d}\mu(p,q)\psi(\mathbf{p},\mathbf{q})\,|\mathbf{p},\mathbf{q}\rangle \otimes |S\rangle, \tag{27}$$

where the spin state $|S\rangle = |\Phi_+\rangle$ and momenta are taken to be entangled Gaussian wave packets of the form

$$\begin{aligned} f_{\Phi+}(\mathbf{p},\mathbf{q},\mathbf{p}_0,\mathbf{q}_0) = [N(\sigma)]^{-\frac{1}{2}}\,[g(\mathbf{p},\mathbf{p}_0)\,g(\mathbf{q},\mathbf{q}_0) \\ +g(\mathbf{p},-\mathbf{p}_0)\,g(\mathbf{q},-\mathbf{q}_0)]\,. \end{aligned} \tag{28}$$

where $N(\sigma)$ is the normalization and $g(\mathbf{p},\mathbf{p}_0)$ a Gaussian of width σ centered at $\mathbf{p}_0 = (p_{x0}, p_{y0}, p_{z0})$,

$$\begin{aligned} g(\mathbf{p},\mathbf{p}_0) = \left[\exp\left(-\frac{(p_x-p_{x0})^2}{2\sigma^2}\right)\exp\left(-\frac{(p_y-p_{y0})^2}{2\sigma^2}\right)\right. \\ \left.\times\exp\left(-\frac{(p_z-p_{z0})^2}{2\sigma^2}\right)\right]^{\frac{1}{2}}. \end{aligned} \tag{29}$$

Boosts are always assumed to be in the z-direction, $\Lambda \equiv \Lambda_z(\xi)$,

$$\Lambda = \begin{pmatrix} \cosh\xi & 0 & 0 & \sinh\xi \\ 0 & 1 & 0 & 0 \\ 0 & 0 & 1 & 0 \\ \sinh\xi & 0 & 0 & \cosh\xi \end{pmatrix}. \tag{30}$$

This implies that the unitary representation of the TWR acting on the one particle subsystem takes the form [37]

$$D[W(\Lambda,\mathbf{p})] = \begin{pmatrix} \alpha & \beta(p_x - \mathrm{i}p_y) \\ -\beta(p_x+\mathrm{i}p_y) & \alpha \end{pmatrix}, \tag{31}$$

where we have denoted

$$\begin{aligned} \alpha &= \sqrt{\frac{E+m}{E^\Lambda+m}}\left(\cosh\frac{\xi}{2} + \frac{p_z}{E+m}\sinh\frac{\xi}{2}\right), \\ \beta &= \frac{1}{\sqrt{(E+m)(E^\Lambda+m)}}\sinh\frac{\xi}{2}, \end{aligned} \tag{32}$$

with ξ being the rapidity of the boost in the z-direction, and

$$E^\Lambda = E\cosh\xi + p_z\sinh\xi. \tag{33}$$

Because the expression of the boosted spin state in is too complex to be tackled by analytic methods, we will resort to numerical treatment in determining the concurrence and the orbits of states. No numerical approximations are involved except for the discretization of the momentum space.

Although we have now specified the generic forms that momenta will take, the particular geometry they might realize is still undetermined. The geometric momenta $\mathbf{p}_0$ and $\mathbf{q}_0$ that specify the centers of Gaussians in $f_{\Phi+}$, Eq. (28), may lie along the same momentum axis, or they may lie along orthogonal axes. They will, correspondingly, generate different types of rotations on the spins. We will next focus on how the generic Gaussian states can be implemented by particular momenta and relate them to different types of rotations generated on spins. To make the discussion perspicuous, we will use discrete momentum states, denoted by $|M\rangle$, that have the same form and subscripts as the continuous ones.

Momenta of both particles may be aligned along the same axes, for instance two particles can be in a superposition of momenta along the x-axis, yielding the state

$$\left|M_{\Phi_+}^{XX}\right\rangle = \frac{1}{\sqrt{2}}\left(|\mathbf{p}_x,\mathbf{q}_x\rangle + |-\mathbf{p}_x,-\mathbf{q}_x\rangle\right). \tag{34}$$

Alternatively, the momenta of both particles may be aligned along different axes, for instance the first particle might be in a superposition of momenta along the x-axis and the second particle in a superposition along the y-axis,

$$\left|M_{\Phi_+}^{XY}\right\rangle = \frac{1}{\sqrt{2}}\left(|\mathbf{p}_x,\mathbf{q}_y\rangle + |-\mathbf{p}_x,-\mathbf{q}_y\rangle\right). \tag{35}$$

Following the assumption (27) above that initially spin and momentum factorize,

$$|\Psi\rangle = |M\rangle \otimes |S\rangle, \tag{36}$$

and substituting momentum $\left|M_{\Phi_+}^{XX}\right\rangle$ into (4) we obtain the boosted state

$$\begin{aligned} \left|\Psi^\Lambda\right\rangle = \frac{1}{2}\Big\{ &|\Lambda_z\mathbf{p}_x,\Lambda_z\mathbf{q}_x\rangle\; D[W(\Lambda_z,\mathbf{p}_x)]\otimes D[W(\Lambda_z,\mathbf{q}_x)] \\ &+|-\Lambda_z\mathbf{p}_x,-\Lambda_z\mathbf{q}_x\rangle\; D[W(\Lambda_z,-\mathbf{p}_x)] \\ &\otimes D[W(\Lambda_z,-\mathbf{q}_x)]\Big\}\,|S\rangle, \end{aligned} \tag{37}$$

where for the sake of concreteness we have taken the boost to be in the z-direction. Now the operators $D[W(\Lambda,\mathbf{p})]$ for the unitary representation of the Wigner rotation in this expression are given in terms of the momenta, the direction of boost and rapidity, that is, variables which specify the configuration of the boost in the physical three space. Formally they are $\mathrm{SU}(2)$ operators parameterized by the latter three quantities. However, as long as our main interest lies in clarifying what

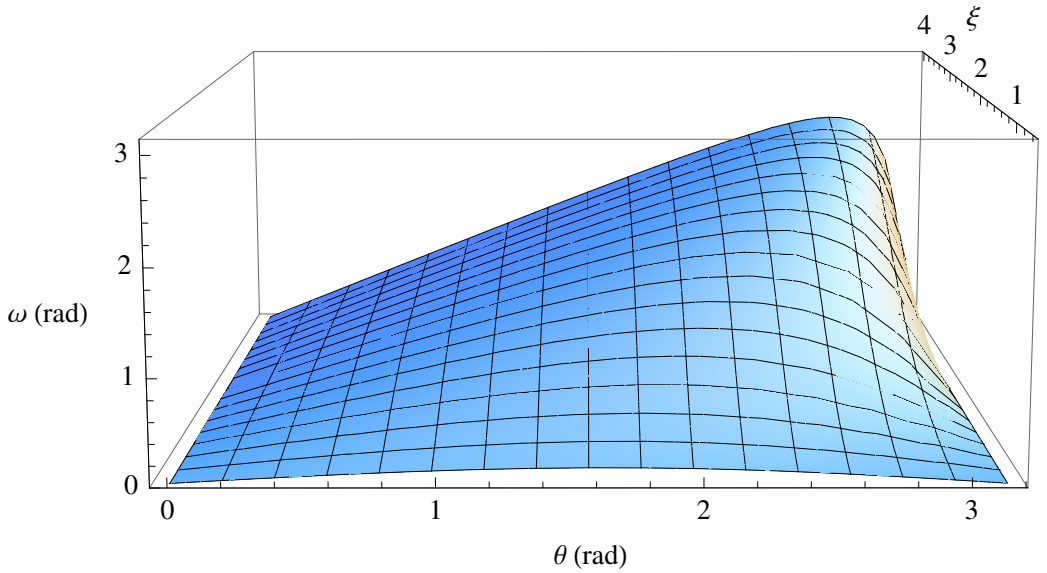

Figure 2. TWR ω as a function of rapidity ξ and boost angle θ.

kind of rotations boosts induce on spins we can simplify the notation and write $R_Y(\omega)$ instead of $D[W(\Lambda_z, \mathbf{p}_x)]$, meaning that the spin is rotated around the y-axis by angle ω. Using this, Eq. (37) can be rewritten as

$$\begin{aligned}\left|\Psi^{\Lambda}\right\rangle =&\frac{1}{2}\big[|\Lambda_z\mathbf{p}_x, \Lambda_z\mathbf{q}_x\rangle\ R_Y(\omega)\otimes R_Y(\chi)\\ &+\ |-\Lambda_z\mathbf{p}_x, -\Lambda_z\mathbf{q}_x\rangle\ R_Y(-\omega)\otimes R_Y(-\chi)\big]\,|S\rangle\,.\end{aligned} \tag{38}$$

Thus we see that the momenta $\left|M^{XX}_{\Phi_+}\right\rangle$ generate rotations of the form

$$R_Y(\pm\omega)\otimes R_Y(\pm\chi), \quad R_Y(\pm\omega)\otimes R_Y(\mp\chi) \tag{39}$$

on the spin state. In the same vein, if the momenta are given by $\left|M^{XY}_{\Phi_+}\right\rangle$ the z-boosted state will have terms that generate rotations

$$R_Y(\pm\omega)\otimes R_X(\pm\chi), \quad R_Y(\pm\omega)\otimes R_X(\mp\chi) \tag{40}$$

on the spin state. Following considerations along these lines we see that by taking momenta along different combinations of axes, one obtains three different types of rotations that can occur on the spin state,

$$\begin{aligned}&\text{(i)}\ \ R_i\otimes\mathbb{1},\\ &\text{(ii)}\ \ R_i\otimes R_i,\\ &\text{(iii)}\ \ R_i\otimes R_j,\quad i\neq j,\end{aligned} \tag{41}$$

where $i, j \in \{X, Y, Z\}$ and each type of rotation can be realized by some set of suitably chosen momenta, see Fig. 3. For instance, we saw that $R_i\otimes R_i$ is instantiated by $R_Y\otimes R_Y$ when the momenta are given by the state $\left|M^{XX}_{\Phi_+}\right\rangle$ and the boost is in the z-direction. Another implementation of the same type is $R_X\otimes R_X$ when the momenta are again entangled but located along the y-axis, $\left|M^{YY}_{\Phi_+}\right\rangle$, and the boost is in the z-direction.

We will next give a few examples of momenta and boost geometries that implement the different types of rotations listed in (41).

a. Type $R_i\otimes\mathbb{1}$. In this scenario, only the first particle undergoes rotation. The momentum of the second particle is chosen so that it leaves the spin alone. Denoting such a momentum by $|0\rangle$, the following pairs of boosts and momenta listed on the left hand side generate rotations given on the right hand side,

$$\begin{aligned}&\Lambda_z\,, |\mathbf{p}_y, 0\rangle \longmapsto R_X\otimes\mathbb{1},\\ &\Lambda_z\,, |\mathbf{p}_x, 0\rangle \longmapsto R_Y\otimes\mathbb{1},\\ &\Lambda_y\,, |\mathbf{p}_x, 0\rangle \longmapsto R_Z\otimes\mathbb{1}.\end{aligned} \tag{42}$$

b. Type $R_i\otimes R_i$. For scenarios in which both particles are rotated around the same axis but not necessarily in the same direction, we obtain the following boosts and momenta,

$$\begin{aligned}&\Lambda_z\,, |\mathbf{p}_y, \mathbf{q}_y\rangle \longmapsto R_X\otimes R_X,\\ &\Lambda_z\,, |\mathbf{p}_x, \mathbf{q}_x\rangle \longmapsto R_Y\otimes R_Y,\\ &\Lambda_y\,, |\mathbf{p}_x, \mathbf{q}_x\rangle \longmapsto R_Z\otimes R_Z.\end{aligned} \tag{43}$$

c. Type $R_i\otimes R_j$, $i\neq j$. Scenarios where particles undergo rotations around different axes can be realized by

$$\begin{aligned}&\Lambda_y\,, |\mathbf{p}_z, \mathbf{q}_x\rangle \longmapsto R_X\otimes R_Z,\\ &\Lambda_z\,, |\mathbf{p}_y, \mathbf{q}_x\rangle \longmapsto R_X\otimes R_Y,\\ &\Lambda_x\,, |\mathbf{p}_z, \mathbf{q}_y\rangle \longmapsto R_Y\otimes R_Z.\end{aligned} \tag{44}$$

These scenarios admit an obvious generalization. By choosing momenta and boosts appropriately, one can consider single particle rotations around an arbitrary axis $\mathbf{n} =$

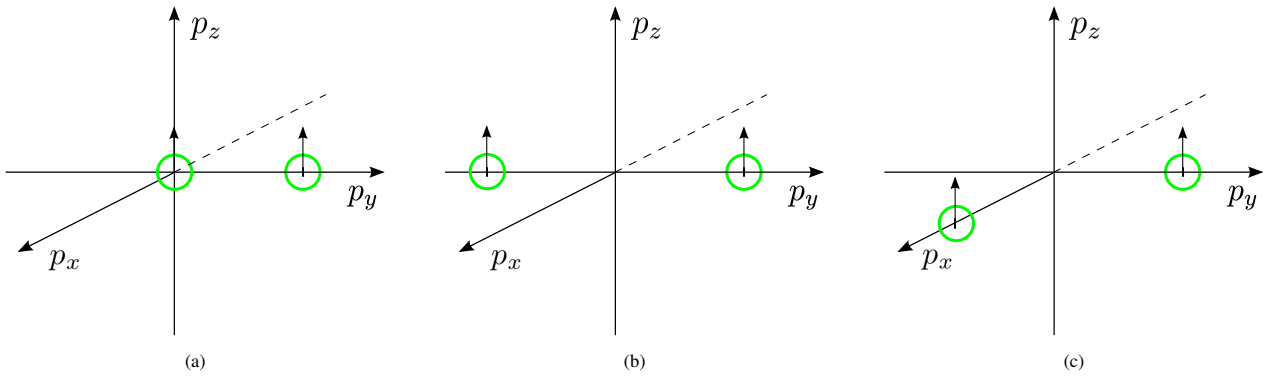

Figure 3. Schematic illustration. Examples of geometric configurations of Gaussian momenta (green circles) for realizations of different types of rotations on spins, with (a) $R_i \otimes \mathbb{1}$, (b) $R_i \otimes R_i$, (c) $R_i \otimes R_j, i \neq j$. The z-projection of the spin field is indicated by an arrow at the Gaussian.

(n_x, n_y, n_z). This leads to combinations of generic rotations $R_{\mathbf{n}_1} \otimes R_{\mathbf{n}_2}$ for two particle systems, opening up a wide avenue of research. However, when surveying the situation for the first time, we would like to keep the scenarios tractable by confining attention to the cases listed above and leave a more general approach for another occasion.

VIII. MOMENTA: TYPE $R_i \otimes \mathbb{1}$

In the following sections we will focus on spin rotations generated by entangled momenta of the form $f_{\Phi+}$. In order to study the maximum range of phenomena that Lorentz boosts can exhibit we will choose boost scenarios with large boost angles and momenta so that the spins undergo large TWR when boosts approach the speed of light. To this end, we will assume that the centers of the Gaussians are given by geometric vectors $\pm\mathbf{p}_{X0} = (\pm 17.13, 0, -98.5)$ and $\pm\mathbf{p}_{Y0} = (0, \pm 17.13, -98.5)$, see Fig. 4. This corresponds to the maxi-

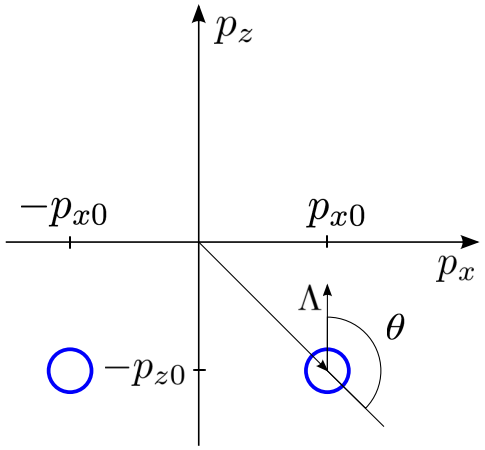

Figure 4. Schematic illustration of a boost at a large angle θ. Gaussian momenta (shown blue) are located at $(\pm p_{x0}, 0, -p_{z0})$. Boost Λ is in the positive z-direction.

mum TWR of 163° at large boosts $\xi = 6.5$.

It is not easy to implement rotations of type $R_i \otimes \mathbb{1}$ in the continuous regime as long as we are concerned with the physical situation where the observer moves relative to both particles. The problem lies in realizing the identity map. Even if we find a scenario where boosts leave alone a momentum given by a delta state, the non-zero width of the wave packet guarantees that this will not apply to the whole wave packet. Some parts of the wave packet will necessarily induce nontrivial transformations on the spin state as we learned in studying the continuous momentum models of a single particle in [17]. We will thus adopt the strategy of constructing a model that approximates the identity map to as high a degree as possible by minimizing the effect of boost on the spin of the second particle.

Above we fixed the boost to be always in the z-direction. In order to realize the $R_i \otimes \mathbb{1}$ rotations, we will take the momentum of the first particle to lie in the zx-plane with $\pm\mathbf{p}_0 = \pm\mathbf{p}_{X0}$, while the momentum of the second particle is located at the origin of the xy-plane with the z-component equal to that of the first particle, $\mathbf{q}_0 = (0, 0, -98.5)$. Since the momentum of the second particle is aligned with the direction of the boost, the resulting rotation of the spin field approximates the identity map.

We plot the orbit of the spin state along with its concurrence in Fig. 5. It is evident that visualization of the orbit provides valuable insight into the behavior of the state, as well as explaining the behavior of entanglement. Let us begin by considering the case $\sigma/m = 1$, shown red in Fig. 5a. Initially the state is at rest, represented by the state $|\Phi_+\rangle$ at the vertex $(1, -1, 1)$. When boosts begin to increase, the state moves towards the center of the face, reaching a separable state $(0, -1, 0)$ at about $\xi = 2.7$. Correspondingly, the concurrence initially takes value 1, decreasing monotonically with the increase of boosts. It vanishes at about $\xi = 2.7$ when the state hits the separable region.

When boosts become larger than 2.7, the spin of the first particle is rotated even further, and the system becomes again entangled, with the orbit moving towards the vertex $(-1, -1, -1)$ which represents the Bell state $|\Psi_-\rangle$. However, the revival of entanglement stops short of reaching the value 0.64 for concurrence. Concurrence starts to decrease when ξ becomes larger than 4.16.

While the states with $\sigma/m = 2$ and $\sigma/m = 4$ display

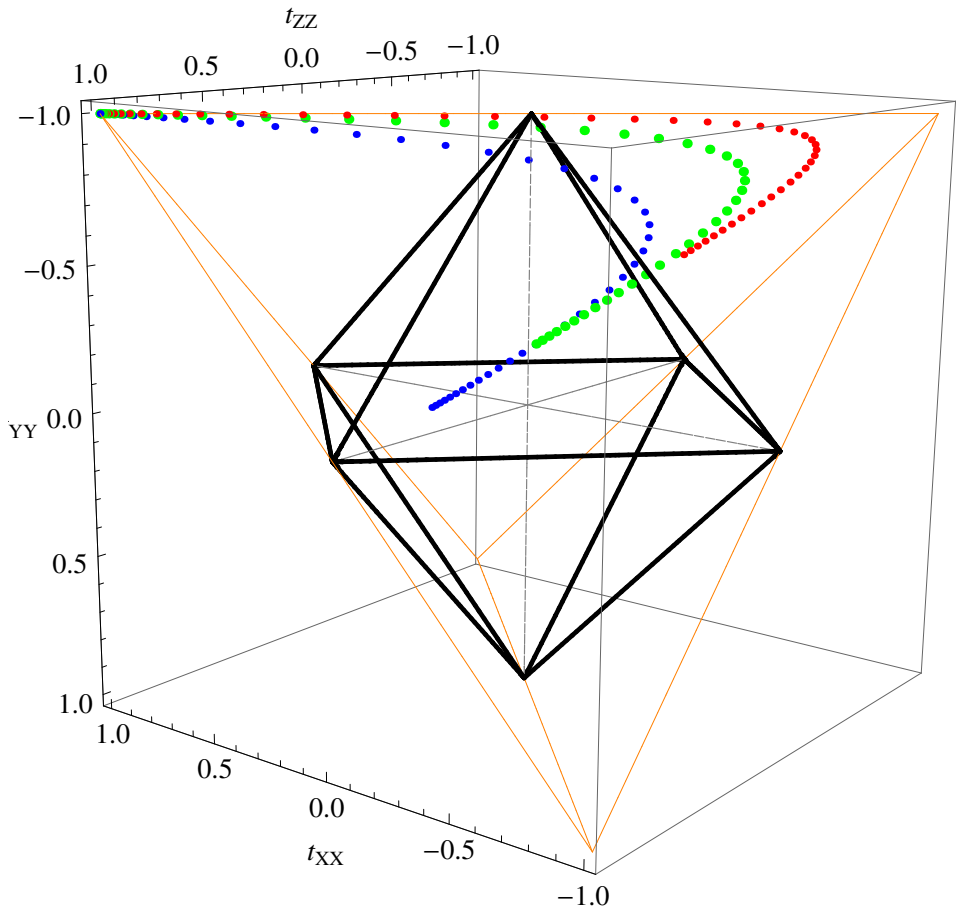

(a)

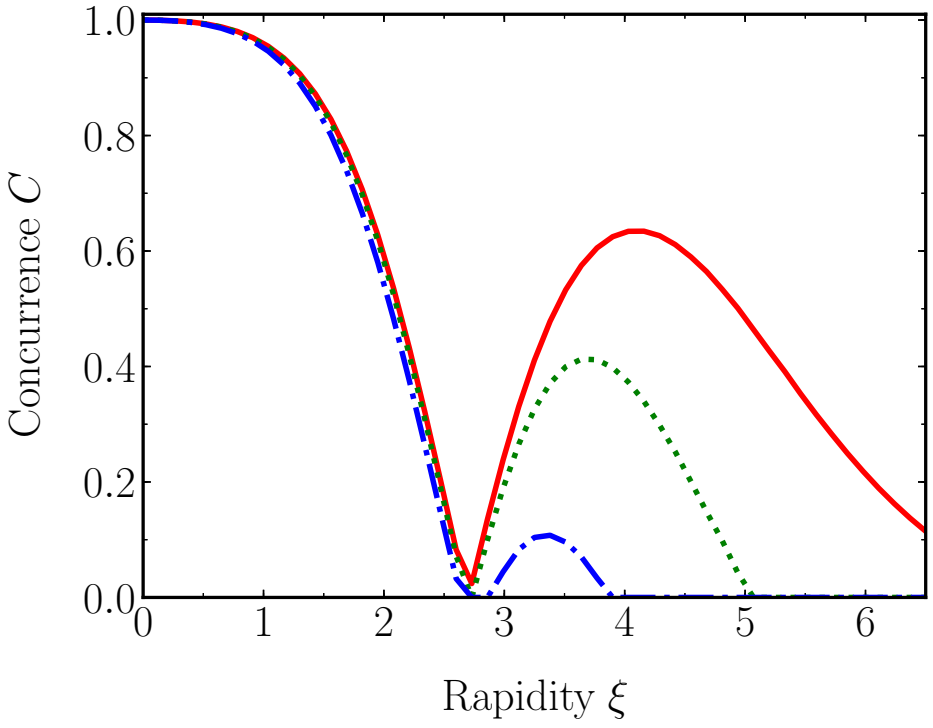

(b)

Figure 5. Spin (a) orbit and (b) concurrence under $R_i \otimes \mathbb{1}$ for Gaussian momenta $f_{\Phi+}$ with $\sigma/m = 1, 2, 4$. (a) Initial state $|\Phi_+\rangle$ corresponds to vertex $(1, -1, 1)$. Data for $\sigma/m = 1$ is shown red, $\sigma/m = 2$ green and $\sigma/m = 4$ blue. (b) Data for $\sigma/m = 1$ is shown as red solid line, $\sigma/m = 2$ as green dotted line and $\sigma/m = 4$ as blue dashed-dotted line.

similar qualitative behavior, their orbits lie increasingly more in the region of separable states as σ/m becomes larger, see Fig. 5a. As a consequence, the revival of concurrence becomes less pronounced, recovering only briefly for $\sigma/m = 4$ in the interval $\xi \in [2.9, 3.9]$ and vanishing thereafter as the state enters the octahedron of separable states.

IX. MOMENTA: TYPE $R_i \otimes R_i$

The case of $R_i \otimes R_i$ realized by entangled momenta falls into two equivalence classes, the trivial and the non-trivial [28]. The former occurs when spins are in an eigenstate of the rotation induced by momenta. We will consider only the interesting, non-trivial case, which can be implemented by $R_X \otimes R_X$. This can be realized by assuming that the Gaussians are centered at the geometric vectors $\pm\mathbf{q}_0 = \pm\mathbf{p}_0 = \pm\mathbf{p}_{Y0}$. We plot the orbits and concurrence for $\sigma/m = 1, 2, 4$ in Fig. 6.

The concurrence exhibits an idiosyncratic double dip behavior. This is clearest seen in the case of $\sigma/m = 1$ and it is due to the fact that the system starts and finishes in nearly the same state, evolving along an orbit that connects the initial state $|\Phi_+\rangle$ at $(1, -1, 1)$ with the state $|\Psi_+\rangle$ at $(1, 1, -1)$. Since it never reaches the initial maximally entangled state, the concurrence saturates at 0.79 at large boosts.

It is interesting to note that the orbit bears some resemblance to the case $R \otimes \mathbb{1}$ in Fig. 5b discussed in the previous section. Similarly to $R \otimes \mathbb{1}$ with $\sigma/m = 1$, the initial state is mapped to $|\Psi_+\rangle$, but in contrast to the single particle rotation, this occurs already at about $\xi = 2.8$ when the rotation reaches $\omega = \pi/2$.

Gaussians with larger widths $\sigma/m = 2$ and $\sigma/m = 4$ diverge from the idealized behavior and end up in increasingly more mixed states for extremely large boosts $\xi = 6.5$ as the width grows. This is to be expected since larger Gaussians contain spins some of which undergo less and others more rotation than spins at the centre of the wave packet, thereby causing the traced out spin state to be a mixed state. Also, larger widths lead to degradation of the double dip pattern as the state does not quite reach $|\Psi_+\rangle$, represented by $(1, 1, -1)$, when $\omega = 90^\circ$, and traverses the top part of the octahedron on its way back to $|\Phi_+\rangle$.

X. MOMENTA: TYPE $R_i \otimes R_j$

In order to realize scenarios where particles undergo rotations around different axis, the centers of Gaussians need to lie in different boost planes. With the boost in the z-direction, we will choose $\pm\mathbf{p}_0 = \pm\mathbf{p}_{Y0}$ and $\pm\mathbf{q}_0 = \pm\mathbf{p}_{X0}$, which means that the spin state is rotated by $R_X \otimes R_Y$. The plot the concurrence is shown in Fig. 7. Unfortunately, the orbit cannot be visualized since it is not Bell diagonal.

It is interesting to note that the concurrence is of the same shape as in the case of the same type of rotation $R_i \otimes R_i$ generated by a product state of the form f_Σ, see the discussion in section X B in [38]. This raises the question of whether the orbit might have the same form as well. However, we can see from Eq. (61) in [28] for the orbit of the corresponding discrete system that this is not the case. While the latter orbit is cyclic in the sense that it returns to the initial state at $\omega = \pi$, the orbit here starts at $|\Phi_+\rangle$ when $\omega = 0$ and ends at $|\Phi_-\rangle$ with $\omega = \pi$.

XI. RELATION TO DISCRETE SYSTEMS

All the cases of continuous momenta discussed above can be related to the discrete systems as follows: when the width of the Gaussian becomes small enough, we observe a good match with discrete systems. For many situations, the behavior of the latter can be calculated analytically [28].

For a concrete example, consider rotations of type $R_i \otimes R_i$ discussed above in section IX. Comparison with the plots of the discrete model, see Fig. 15 in [28], shows that for $\sigma/m = 1$ the behavior of the continuous and the discrete model coincide to quite a high degree of accuracy. The orbit of the continuous system follows the same path as the discrete one, almost reaching the rest frame state $|\Phi_+\rangle$. The reason it stops short of $|\Phi_+\rangle$ is that while in the discrete model we assume that the system reaches the maximum TWR of 180°, the maximum rotation implemented by the continuous model at $\xi = 6.5$ is $\omega_m \approx 163^\circ$ or 2.81 rad. Substituting ω_m into the expression that describes the discrete orbit, Eq. (77) in [28], yields $t_{X\otimes X}(\omega_m) = (1.00, -0.79, 0.79)$, which is in good agreement with the numerically calculated value $(0.99, -0.79, 0.80)$ representing the final state for $\sigma/m = 1$ in Fig. 6. Likewise, the concurrence of the discrete model, Eq. (62) with $\lambda = 1$ in [28], evaluates to $C(\omega_m) = 0.79$, showing again good fit with the numerically computed value 0.79 of the continuous model.

This generic pattern can be shown to hold for each type of rotation. While one might think that the case $R_i \otimes \mathbb{1}$ in section VIII provides a counterexample, this is not true. The reason it deviates from the discrete behavior is that the identity map can not be implemented accurately enough. Realistic systems that are characterized by wave packets of finite width always contain momenta which induce some rotation on the spin field, thereby diverging from idealized behavior.

XII. CONCLUSION

We have explored spin entanglement of two particles in relativity. While previous work has studied discrete states [28] that represent idealized models, realistic situations involve states whose momenta are given by continuous distributions. In order to understand how relaxing idealization affects the behavior of entanglement we assumed that momenta are given by entangled Gaussians while spins were in the maximally entangled Bell state $|\Phi_+\rangle$.

The overall lesson emerging is that relativistic entanglement in inertial frames is observer dependent [18]. However, no single conclusion can be drawn about how entanglement

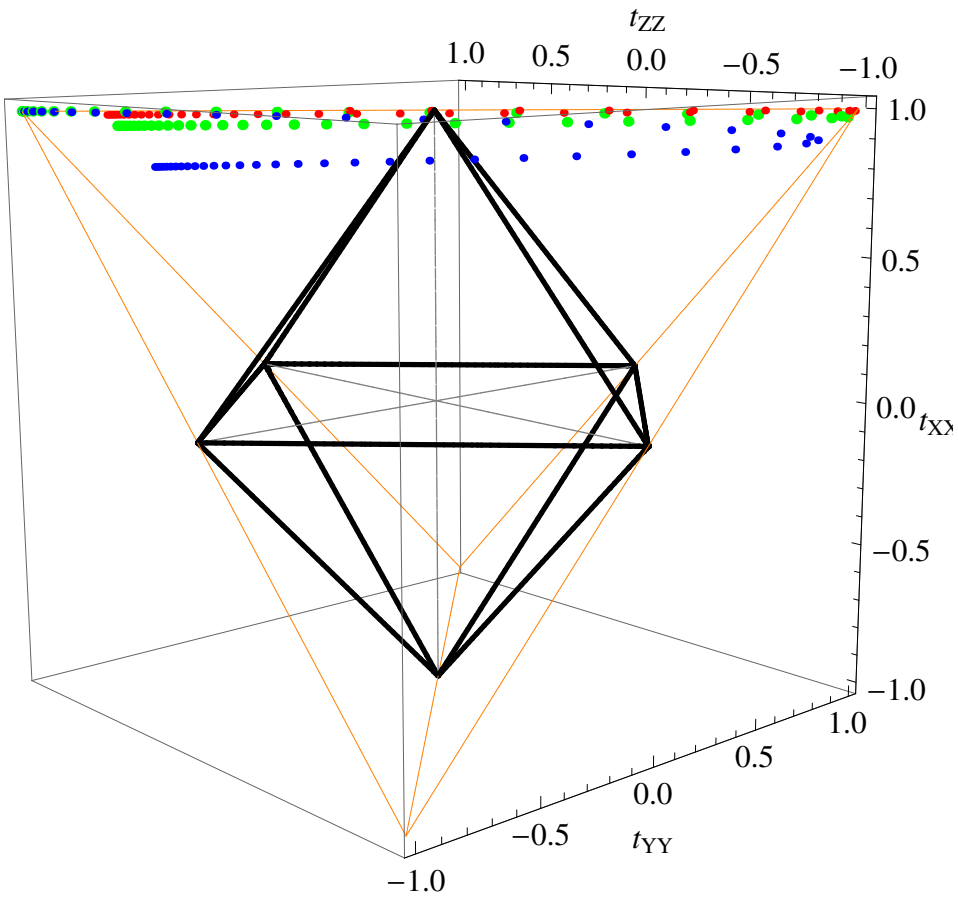

(a)

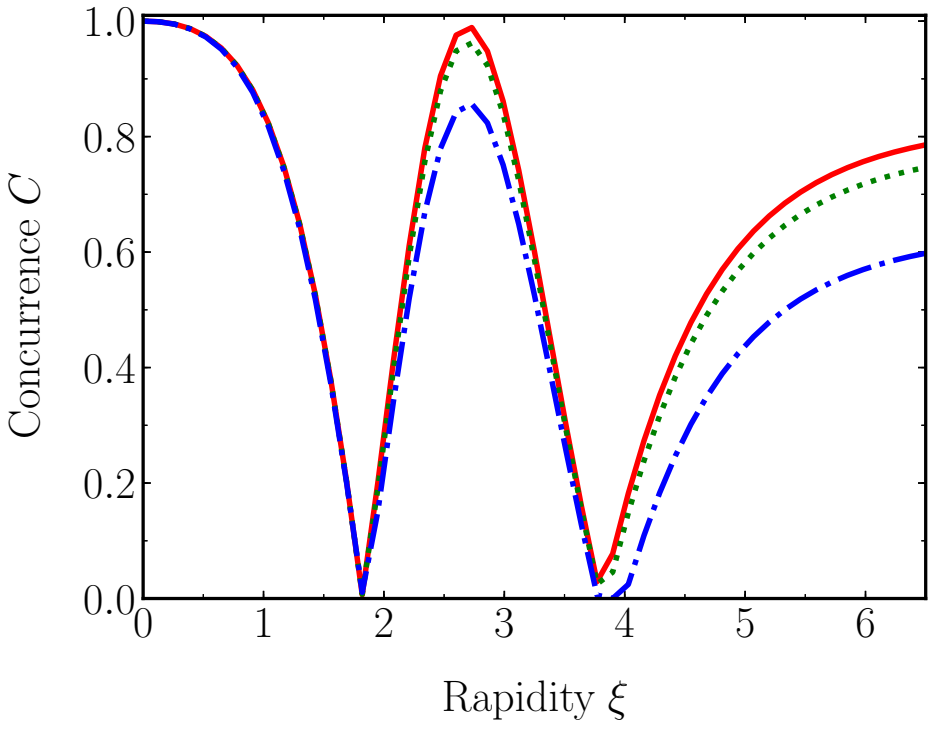

(b)

Figure 6. Spin (a) orbit and (b) concurrence under $R_i \otimes R_i$ for entangled Gaussian momenta with $\sigma/m = 1, 2, 4$. Momenta are given by $f_{\Phi+}$. (a) Initial state $|\Phi_+\rangle$ corresponds to vertex $(1, -1, 1)$. Data for $\sigma/m = 1$ is shown red, $\sigma/m = 2$ green and $\sigma/m = 4$ blue. (b) Data for $\sigma/m = 1$ is shown as red solid line, $\sigma/m = 2$ as green dotted line and $\sigma/m = 4$ as blue dashed-dotted line.

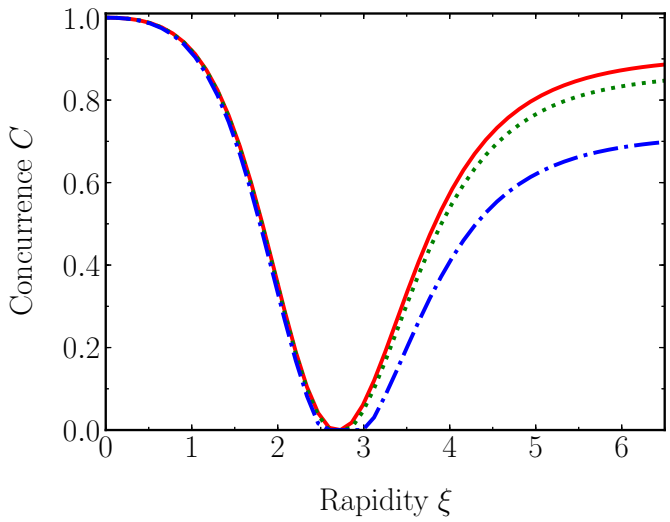

Figure 7. Spin concurrence under $R_i \otimes R_j, i \neq j$ for entangled Gaussian momenta with $\sigma/m = 1, 2, 4$. Momenta are given by $f_{\Phi+}$. Data for $\sigma/m = 1$ is shown as red solid line, $\sigma/m = 2$ as green dotted line and $\sigma/m = 4$ as blue dashed-dotted line.

changes. Instead, we witness different behaviors of spin entanglement which depend on the boost situation at hand, i.e. the momentum state and its geometry. Aside from the trivial case where entanglement is left invariant, most scenarios we studied led to significant changes of concurrence. The trivial case is exemplified by $R_Y \otimes R_Y$ where the spins are in the eigenstate of the rotation generated by momenta. On the other hand, another instance of the same type, $R_X \otimes R_X$, shows rapid change of concurrence as rapidity varies between zero and the maximum value.

Although our results were obtained by numerical computations, we explained how one can understand the behavior of continuous momenta by modelling them in terms of discrete momentum states. The picture is one where systems involving continuous momenta can be conceived of as spin fields at a large number of discrete momenta. Boosting means that each spin undergoes a different momentum dependent rotation for a fixed value of rapidity. The difference between the above mentioned two cases, where the first one shows almost no change in entanglement whereas the other ranges significantly, can be explained in terms of rotations induced in the dicrete model on the spin degrees of freedom.

Our model assumed that the spin and momentum degrees of freedom factorize. Yet this is less of a restriction when one realizes that spin–momentum entangled states have been, to some extent, implicit in the investigation too. The reason is that all inertial frames are equivalent and Lorentz boosts are group elements, meaning that we are guaranteed to have inverse elements and the scenarios can be read in the reverse direction. One can regard the final state, which typically contains spin–momentum entanglement, as the rest frame state, and take the inverse boost to obtain the initial state. For instance, consider the boosted state at $\xi = 1.8$ in Fig. 6a, which is represented by the point $(0.9, 0, 0)$. Applying the inverse boost gives back the original maximally entangled Bell state $|\Phi_+\rangle$. Importantly, this points to an asymmetry between spin–momentum product versus entangled states. While the latter can lead to an increase of spin–spin entanglement, it has been shown that the former can never cause such behavior [2].

We would finally like to stress the usefulness of visualizing spin orbits. It provided geometric insight into the behavior of entanglement by showing how states follow regions of different classes of entanglement. This enables a more detailed understanding of how varying the initial states, their widths and momenta, changed the spin concurrence. The hope is that the results obtained in this paper contribute to a better understanding of entanglement in relativity and could lead to future applications which might be of interest in relativistic quantum information.

XIII. ACKNOWLEDGMENTS

Veiko Palge was supported by EU through the ERDF CoE program grant TK133 and by the Estonian Research Council via IUT2-27. Stefan Groote and Hannes Liivat were supported by the Estonian Research Council via IUT2-27. We would like to thank Hardi Veermäe for many helpful suggestions.

Appendix A: Wigner representation

1. Conventions

We will use natural units where $\hbar = c = 1$. Spacetime metric is $\mathrm{diag}(+---)$. Latin indices i, j, k etc. take values in three tuples (x, y, z) or $(1, 2, 3)$ while Greek indices μ, ν etc. run over (t, x, y, z) or $(0, 1, 2, 3)$. Three vectors use boldface whereas four vectors are given in ordinary type. For instance, the four momentum is $p^\mu = (p^0, \mathbf{p})$ with the norm $p^\mu p_\mu = (p^0)^2 - \mathbf{p}^2 = m^2$.

2. Particles in the Wigner representation

In this section, we summarize the background for the relativistic quantum mechanical constructions used in the paper. Free spin-$1/2$ particles can be described in two different theories, the unitary irreducible representation of the Poincaré group or in the Dirac theory of bispinors [39]. Throughout we will work in the Wigner representation (also called the Wigner-Bargmann or the spin basis) which can be found in references [25, 29, 30]. The single particle states are given by a unitary irreducible representation of the Poincaré group where a representation is labelled by mass $m > 0$ and the intrinsic spin s which takes integral or half-integral values. The representation can be realized in the space $\bigoplus^{2s+1} L^2(\Gamma_m^+)$ of square integrable functions on the forward mass hyperboloid $\Gamma_m^+ = \{p \in \mathbf{M} : p^2 = m^2, p^0 > 0\}$ where the scalar product is defined as

$$\langle \phi | \psi \rangle = \sum_\sigma \int \mathrm{d}\mu(p)\, \phi_\sigma^*(p) \psi_\sigma(p), \tag{A1}$$

with $\mathrm{d}\mu(p) = [2E(\mathbf{p})]^{-1}\mathrm{d}^3\mathbf{p}$ being the Lorentz invariant integration measure. In this paper we specialize on spin-$1/2$ systems. In this case the state space is given by

$$\mathcal{H} = L^2(\mathbb{R}^3) \oplus L^2(\mathbb{R}^3) = L^2(\mathbb{R}^3, \mathbb{C}^2) = L^2(\mathbb{R}^3) \otimes \mathbb{C}^2. \tag{A2}$$

In order to define basis vectors, we start by specifying the rest frame states in terms of the four momentum P^μ, the square of total angular momentum $\mathbf{J}^2$ and the z-component of the angular momentum J_z,

$$\begin{aligned} P^\mu \left|\mathbf{0}, \lambda\right\rangle &= p_0^\mu \left|\mathbf{0}, \lambda\right\rangle \\ \mathbf{J}^2 \left|\mathbf{0}, \lambda\right\rangle &= s(s+1) \left|\mathbf{0}, \lambda\right\rangle \\ J_z \left|\mathbf{0}, \lambda\right\rangle &= \lambda \left|\mathbf{0}, \lambda\right\rangle, \end{aligned} \tag{A3}$$

where $\mathbf{0}$ denotes $\mathbf{p} = 0$ with $p_0^\mu = (m, \mathbf{0})$, and we have abbreviated $|\mathbf{p}, \lambda\rangle = |\mathbf{p}\rangle \otimes |\lambda\rangle$. Because the particle is at rest, s and λ refer to the spin and the z-component of the particle. We next generate a complete basis, which consists of the general eigenvectors of P^μ, by acting on the rest frame state with a pure, rotation free Lorentz boost,

$$\left|\mathbf{p}, \lambda\right\rangle = U[L(\mathbf{p})] \left|\mathbf{0}, \lambda\right\rangle \tag{A4}$$

where $U[L(\mathbf{p})]$ is a unitary representation of the boost $L(\mathbf{p})$ that takes the rest momentum $(m, \mathbf{0}) = p_0$ to an arbitrary momentum,

$$L(\mathbf{p})\,(m, \mathbf{0}) = (E(\mathbf{p}), \mathbf{p}), \tag{A5}$$

with $E(\mathbf{p}) = \sqrt{\mathbf{p}^2 + m^2}$. The basis vectors $|\mathbf{p}, \lambda\rangle$ span the single particle state space $\mathcal{H}$ and we can write a generic state as

$$\left|\Psi\right\rangle = \sum_\sigma \int \mathrm{d}\mu(p)\, \psi_\sigma(\mathbf{p}) \left|\mathbf{p}, \sigma\right\rangle, \tag{A6}$$

The basis states are normalized as follows,

$$\langle \mathbf{p}', \sigma' | \mathbf{p}, \sigma \rangle = 2E(\mathbf{p}) \delta^3(\mathbf{p} - \mathbf{p}') \delta_{\sigma\sigma'}. \tag{A7}$$

The action of a generic Lorentz transformation Λ on basis element is given by

$$U(\Lambda) \left|\mathbf{p}, \sigma\right\rangle = \sum_\lambda \left|\Lambda\mathbf{p}, \lambda\right\rangle D_{\lambda\sigma}[W(\Lambda, \mathbf{p})], \tag{A8}$$

where $W(\Lambda, \mathbf{p})$ is the Wigner rotation,

$$W(\Lambda, \mathbf{p}) \equiv L^{-1}(\Lambda\mathbf{p}) \Lambda L(\mathbf{p}) \tag{A9}$$

that leaves p_0 invariant, $p_0 = W p_0$. For massive particles, $W \in \mathrm{SO}(3)$ is a rotation and $D[W(\Lambda, \mathbf{p})]$ is its representation. For spin-$1/2$ particles, the latter is an element of $\mathrm{SU}(2)$, whose concrete form in terms of momenta and rapidities can be found in [37].

3. Lorentz transformations on particles

One can now calculate the transformation on the wave function. In the Lorentz boosted frame the state is $\left|\Psi^\Lambda\right\rangle = U(\Lambda) \left|\Psi\right\rangle$, so we have

$$\begin{aligned} \left|\Psi^\Lambda\right\rangle &= \sum_\sigma \int \mathrm{d}\mu(p)\, \psi_\sigma(\mathbf{p}) \sum_\lambda \left|\Lambda\mathbf{p}, \lambda\right\rangle D_{\lambda\sigma}[W(\Lambda, \mathbf{p})] \\ &= \sum_\lambda \int \mathrm{d}\mu(p')\, \sum_\sigma D_{\lambda\sigma}[W(\Lambda, \Lambda^{-1}\mathbf{p}')] \psi_\sigma(\Lambda^{-1}\mathbf{p}') \left|\mathbf{p}', \lambda\right\rangle \\ &= \sum_\lambda \int \mathrm{d}\mu(p)\, \psi^\Lambda_\lambda(\mathbf{p}) \left|\mathbf{p}, \lambda\right\rangle, \end{aligned} \tag{A10}$$

where $\mathbf{p}' = \Lambda\mathbf{p}$ and we used the fact that the integration measure is Lorentz covariant, $\mathrm{d}\mu(p) = \mathrm{d}\mu(\Lambda p)$, with a relabelling $\mathbf{p}' \to \mathbf{p}$ of dummy variables in the last line. Hence we have,

$$\psi^\Lambda_\lambda(\mathbf{p}) = \sum_\sigma D_{\lambda\sigma}[W(\Lambda, \Lambda^{-1}\mathbf{p})] \psi_\sigma(\Lambda^{-1}\mathbf{p}). \tag{A11}$$

The state of a two particle system belongs to $\mathcal{H}_2 = \mathcal{H}_1 \otimes \mathcal{H}_1$ where $\mathcal{H}_1$ is the one particle Hilbert space described above. A Lorentz boost Λ acts on the two particle state by $U(\Lambda) \otimes U(\Lambda)$ and in analogy to the single particle case we calculate that the corresponding transformation of the wave function is given by

$$\begin{aligned} \psi^\Lambda_{\lambda\kappa}(\mathbf{p}, \mathbf{q}) = \sum_{\sigma,\xi} D_{\lambda\sigma}\left[W(\Lambda, \Lambda^{-1}\mathbf{p})\right] D_{\kappa\xi}\left[W(\Lambda, \Lambda^{-1}\mathbf{q})\right] \\ \times \psi_{\sigma\xi}(\Lambda^{-1}\mathbf{p}, \Lambda^{-1}\mathbf{q}). \end{aligned} \tag{A12}$$

[1] M. Czachor, Physical Review A **55**, 72 (1997).
[2] R. M. Gingrich and C. Adami, Physical Review Letters **89**, 270402 (2002).
[3] A. Peres, P. F. Scudo, and D. R. Terno, Physical Review Letters **88**, 230402 (2002).
[4] P. M. Alsing and G. J. Milburn, Quantum Information and Computation **2**, 487 (2002).
[5] D. Ahn, H.-J. Lee, and S. W. Hwang, arXiv:quant-ph/0207018 (2002).
[6] D. Ahn, H.-J. Lee, Y. H. Moon, and S. W. Hwang, Physical Review A **67**, 012103 (2003).
[7] D. Ahn, H.-J. Lee, and S. W. Hwang, Physical Review A **67**, 032309 (2003).
[8] M. Czachor and M. Wilczewski, Physical Review A **68**, 010302 (2003).
[9] Y. H. Moon, S. W. Hwang, and D. Ahn, Progress of Theoretical Physics **112**, 219 (2004).
[10] D. Lee and E. Chang-Young, New Journal of Physics **6**, 67

(2004).
[11] M. Czachor, Physical Review Letters **94**, 078901 (2005).
[12] L. Lamata, M. A. Martin-Delgado, and E. Solano, Physical Review Letters **97**, 250502 (2006).
[13] P. M. Alsing, I. Fuentes-Schuller, R. B. Mann, and T. E. Tessier, Physical Review A **74**, 032326 (2006).
[14] A. Chakrabarti, Journal of Physics A: Mathematical and Theoretical **42**, 245205 (2009).
[15] I. Fuentes, R. B. Mann, E. Martín-Martínez, and S. Moradi, Physical Review D **82**, 045030 (2010).
[16] N. Friis, R. A. Bertlmann, and M. Huber, Physical Review A **81**, 042114 (2010).
[17] V. Palge and J. Dunningham, Physical Review A **85**, 042322 (2012).
[18] P. M. Alsing and I. Fuentes, Classical and Quantum Gravity **29**, 224001 (2012).
[19] H. Terashima and M. Ueda, International Journal of Quantum Information **01**, 93 (2003).
[20] P. Caban and J. Rembieliński, Physical Review A **72**, 012103 (2005).
[21] P. Caban and J. Rembieliński, Physical Review A **74**, 042103 (2006).
[22] T. Jordan, A. Shaji, and E. Sudarshan, Physical Review A **73**, 032104 (2006).
[23] T. Jordan, A. Shaji, and E. Sudarshan, Physical Review A **75**, 022101 (2007).
[24] V. Palge, V. Vedral, and J. A. Dunningham, Physical Review A **84**, 044303 (2011).
[25] P. Caban, J. Rembieliński, and M. Włodarczyk, Physical Review A **88**, 022119 (2013).
[26] We will use the abbreviation TWR in honor of Thomas's contribution of discovering the Thomas precession [40, 41].
[27] A related study explores the situation where momenta are given by separable states involving combinations of Gaussians [38].
[28] V. Palge and J. Dunningham, Annals of Physics **363**, 275 (2015).
[29] R. U. Sexl and H. K. Urbantke, *Relativity, Groups, Particles: Special Relativity and Relativistic Symmetry in Field and Particle Physics*, rev. ed. ed. (Springer, New York, 2001).
[30] N. N. Bogolubov, A. A. Logunov, and I. T. Todorov, *Introduction to Axiomatic Quantum Field Theory* (W.A.Benjamin, 1975).
[31] A. J. MacFarlane, Journal of Mathematical Physics **4**, 490 (1963).
[32] W. Wootters, Physical Review Letters **80**, 2245 (1998).
[33] From a more general perspective, it is interesting to consider mixed states as well. See [28] for an extension to the Werner states.
[34] I. Bengtsson and K. Życzkowski, *Geometry of Quantum States: An Introduction to Quantum Entanglement* (Cambridge University Press, 2006).
[35] R. A. Bertlmann, H. Narnhofer, and W. Thirring, Physical Review A **66**, 032319 (2002).
[36] J. A. Rhodes and M. D. Semon, Am. J. Phys. **72**, 943 (2004).
[37] F. R. Halpern, *Special Relativity and Quantum Mechanics* (Prentice-Hall, 1968).
[38] V. Palge, J. Dunningham, S. Groote, and H. Liivat, arXiv:1409.1316 [quant-ph] (2014), arXiv: 1409.1316.
[39] The unitary irreducible representation is due to Wigner [42]. A standard treatment of the two representations is given by [30]. See [43] for a very readable account on the relationship between the two frameworks and [25] for a discussion in the context of spin observable in the Dirac theory.
[40] L. H. Thomas, Nature **117**, 514 (1926).
[41] L. H. Thomas, Philosophical Magazine 7, **3**, 1 (1927).
[42] E. Wigner, Annals of Mathematics Second Series, **40**, 149 (1939).
[43] W. N. Polyzou, W. Glöckle, and H. Witała, Few-Body Systems **54**, 1667 (2012).